Minimal Peptide Length for Interaction of Amphipathic α-Helical Peptides with Phosphatidylcholine Liposomes

Larry R. McLean,* Karen A. Hagaman, Thomas J. Owen, and John L. Krstenansky
Merrell Dow Research Institute, 2110 East Galbraith Road, Cincinnati, Ohio 45215
Received April 18, 1990; Revised Manuscript Received September 7, 1990

ABSTRACT: The interactions of a series of amphipathic α-helical peptides containing from 6 to 18 amino acid residues with dipalmitoylphosphatidylcholine (DPPC) and dimyristoylphosphatidylcholine (DMPC) were studied by optical and calorimetric methods. Several peptides rapidly decreased the turbidity of DMPC and DPPC liposomes when mixed at the phase transition temperatures of the lipids. The extent of the clearing depended upon the chain length of the peptides, with the most effective clearing attained with peptides 10–12 residues in length. An eight-residue peptide was somewhat less effective and a six-residue peptide had no effect on liposome structure. The peptides formed small micellar structures, as judged by gel filtration chromatography. The effects of the peptides on the phase transitions of the lipids were examined by differential scanning calorimetry. The peptides that were most effective in disrupting the liposomes and forming clear micelles were also most effective in reducing the enthalpy of the gel to liquid-crystalline phase transition of the lipid. The addition of DMPC or DPPC liposomes to the peptides increased the magnitude of the negative bonds at 208 and 222 nm in circular dichroism measurements, consistent with the expected formation of α-helical structure on binding to lipid. The extent of burial of the single tryptophan residue in the peptides was determined by fluorescence spectroscopy. In peptides that bound to lipid, the tryptophan was in a less solvent-exposed environment in the presence of lipid, as evidenced by a blue shift in the fluorescence emission maximum of the peptide. The effectiveness of the peptides in forming clear micellar structures from liposomes was related to the hydrophobic surface area of the peptides. An optimal surface area of 6–7.5 nm^2 was found for peptides most effective in liposome clearing. The free energy of transfer of this surface from an aqueous phase to nonpolar phase is just sufficient to exceed the unfavorable increase in free energy associated with restriction of the peptide to two dimensions in the peptide–lipid micelle. These data demonstrate that an effective lipid-binding amphipathic α-helix need only be 18 residues in length.

The amphipathic α-helix is a common structural feature in many proteins that bind to phospholipids and in several peptide hormones and cytotoxic peptides (Segrest et al., 1974; Kaiser & Kezdy, 1984; Argiolas & Pisano, 1985). The amphipathic α-helix is defined as an α-helical region of a protein in which the amino acid residues are distributed in the secondary structure to form opposing polar and nonpolar faces. In peptide hormones, the amphipathic α-helix is thought to play an important role, possibly by interacting with lipid in the membrane or with an amphipathic α-helical region within the receptor. In addition, certain amphipathic α-helical peptides are effective antiviral agents (Srinivas et al., 1990) or may be mixed with DPPC[1] to form a synthetic lung surfactant (McLean et al., 1990). Although considerable effort has been expended in designing peptide hormones that contain amphipathic α-helical regions within their sequence, less attention has been paid to the structural features within the amphipathic α-helical motif that are required for lipid interaction.

We have designed a series of model amphipathic α-helical peptides (MAP) utilizing amphipathic analysis and several means of α-helical stabilization in order to produce short, highly α-helical peptides (Krstenansky et al., 1989). The sequences of the novel MAPs are based on a repeating 11 amino acid sequence, Glu-Leu-Leu-Glu-Lys-Leu-Leu-Glu-Lys-Leu-Lys, designated as MAP_{1-11}. A large part of the impetus for designing such a sequence was to provide a regular sequence in which the residues may be systematically varied in order to probe the effects of charge distribution, the size and shape of the hydrophobic region of the peptide, and of peptide length. In order to place such studies on a sure footing, we began by examining the effect of peptide length on the interaction of the peptides with lipid, hoping to find the shortest peptide that retained the salient features of the amphipathic α-helix and that could be readily and systematically modified.

Interaction of amphipathic α-helical peptides and proteins with DMPC or DPPC liposomes generally leads to disruption of the vesicular structure of the liposomes, resulting in the formation of disk-shaped micelles containing peptide and lipid (Morrisett et al., 1977). Associated with this peptide–lipid interaction, an increase in the α-helicity and a decrease in the solvent exposure of tryptophan is observed. In addition, the phase transition of the lipid is reduced in enthalpy. These physical effects are characteristic of lipid-binding interactions in amphipathic α-helical peptides and are good criteria to judge the nature and extent of the lipid–protein interaction. In the present report, such structural features of the lipid and the peptide within the micelles were examined to find the optimal length for a lipid-binding peptide in the MAP series.

Experimental Procedures

Materials. Peptides were synthesized on a 0.5-mmol scale by solid-phase methods on an Applied Biosystems Inc. (Foster City, CA) Model 430-A peptide synthesizer as described previously (Krstenansky et al., 1989). The purity and identity of the peptides were confirmed by analytical high-performance liquid chromatography (HPLC), amino acid analysis, and fast atom bombardment mass spectrometry (FAB-MS). Dipalmitoylphosphatidylcholine (DPPC) and dimyristoyl-

* Address correspondence to this author.

[1] Abbreviations: DPPC, dipalmitoylphosphatidylcholine; DMPC, dimyristoylphosphatidylcholine; TFE, trifluoroethanol.

0006-2960/91/0430-31$02.50/0

Table I: Sequences, Trivial Names, and Liposome Clearing of Peptides[a]

name	length	sequence	A_{400}
WMAP18	18	Suc K L L E K L K E L L E K L L E W L K #	0.108
W9MAP17	17	Suc K L K E L L E K L L E W L K E L L #	0.072
WMAP14	14	Suc K L K E L L E K L L E W L K #	0.034
WMAP12	12	Mpa K E L L E K L L E W L K #	0.004
WMAP11	11	6-Ahx E L L E K L L E W L K #	0.003
WMAP10	10	Suc L L E K L L E W L K #	0.007
W9MAP10	10	Suc K L L E W L K E L L #	0.012
WMAP8	8	Mpa E K L L E W L K #	0.059
WMAP6	6	6-Ahx L L E W L K #	0.136

[a] Peptides were added to DPPC liposomes (0.16 mg/mL in 2 mL of buffer) at 42.0 ± 0.2 °C to attain a weight ratio of 1:2 peptide/DPPC. The mixture was stirred and incubated for 30 min, and then the absorbance was recorded at 400 nm. The initial A_{400} of the liposomes was 0.142–0.146. Abbreviations: E, glutamic acid; K, lysine; L, leucine; W, tryptophan; Suc, succinimide (desamino Asp); Mpa, methylpentanoic acid (desamino Leu); 6-Ahx, 6-aminohexanoic acid (desamino Lys); #, amide.

phosphatidylcholine (DMPC) were purchased from Avanti Polar Lipids (Birmingham, AL).

Preparation of Peptide–Lipid Mixtures. Liposomes were prepared by dissolving 4 mg of DPPC or DMPC in chloroform, drying the lipid under N_2 and for 30–60 min under vacuum, and incubating the lipid in 2 mL of 10 mM Tris-HCl, pH 7.4, for 1 h at 45–50 °C (DPPC) or 37 °C (DMPC) with occasional vortexing. The resulting turbid liposomes were diluted to 0.16 mg/mL in 2 mL of buffer. Then peptide (4 mg/mL in 6 M guanidine hydrochloride or dry) was added to attain a given weight ratio of peptide to lipid and the samples were incubated at 42 °C for DPPC and 24 °C for DMPC overnight. For spectroscopic measurements, samples that did not clear in an overnight incubation were bath sonicated (Branson 1200) until clear (30 min to 2 h) and then incubated overnight.

Differential Scanning Calorimetry. DSC was performed on a Microcal MC-2 differential scanning calorimeter at a scan rate of 1 °C/min. Sample concentrations were 0.1–0.2 mg/mL. The differential voltage signal from the thermopiles, the temperature of the heat sink, and the time were recorded at 10-s intervals on an IBM-PC-AT computer. The data were converted to cal/g·°C after dividing by the scan rate and the weight of sample. Enthalpies were calculated by numerical integration; the phase transition temperatures (T_m) correspond to the temperatures at which the heat capacities reach maximum values during the transitions.

Spectra. Fluorescence spectra were recorded on an SLM 4800 spectrofluorometer under a N_2 atmosphere at 25 °C. Emission spectra were recorded with an excitation wavelength of 280 nm. Circular dichroic (CD) spectra of samples in 1-mm circular cuvettes were recorded at room temperature on a Jasco J-500A spectropolarimeter with 2-nm slit width. The CD spectrum of buffer was subtracted from the CD spectrum of the sample after each scan. The scan rate was 2 nm/min and the time constant was 8 s. Data were collected at 0.04-nm intervals and averaged over a 0.2-nm interval. For calculation of molar ellipticities, the molecular weight of the peptide was divided by the number of residues plus one to account for the N-terminal des-amino acid and the C-terminal amide, which are not counted as residues in Table I.

Results

The sequences of the model amphipathic α-helical peptides (MAPs) are based on a repeating 11 amino acid sequence, Glu-Leu-Leu-Glu-Lys-Leu-Leu-Glu-Lys-Leu-Lys. Table I shows the sequences of the peptides that were synthesized. The various peptides represent different lengths and two "phases" of the MAP sequence, where the phase corresponds to the position of the final residue in the repeating sequence. Both the N- and C-termini are neutral. This is accomplished with a C-terminal amide and a des-amino residue at the N-terminus, where succinyl (Suc) replaces Glu, methylpentanoic acid (Mpa) replaces Leu, and 6-aminohexanoic acid (6-Ahx) replaces Lys. A single Trp residue replaces one of the Lys residues in the repeating sequence to allow fluorescence measurements on the peptides. The position of the Trp is at the edge of the hydrophobic face of the peptide [position 9 in MAP_{1-11} (Krstenansky et al., 1989)] so is not expected to significantly alter the amphipathic α-helical nature of the peptides.

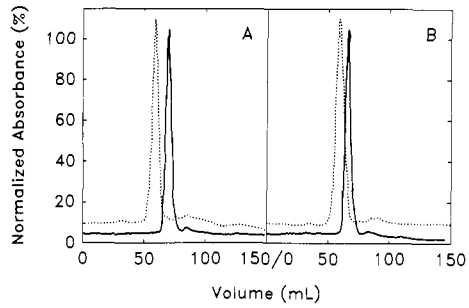

FIGURE 1: Gel filtration chromatography of mixtures of (A) WMAP18 and (B) WMAP14 with DMPC at ratios of 1:1 (—) and 1:5 (···) (peptide/lipid by weight). A Superose 6B preparative column (16 × 50 cm) was loaded with 0.75 mL of the peptide–lipid mixtures. The effluent was monitored by absorbance at 280 nm; the flow rate was 0.5 mL/min. The void volume of the column was 32.0 mL; the end volume was 84.8 mL. The elution volumes (mL) were the following: WMAP18/DMPC 1:5, 59.0; WMAP18/DMPC 1:1, 66.2; WMAP10/DMPC 1:5, 59.3; WMAP10/DMPC 1:1, 69.8.

Interaction of Peptide with Lipid. Addition of several of the peptides to DMPC or DPPC liposomes results in a relatively rapid decrease in the turbidity of the liposomes. After 30 min of incubation at 42 °C for DPPC, the A_{400} of the samples is reduced to the values listed in Table I. Similar data were obtained with DMPC liposomes and incubation at 24 °C. On the basis of the values of A_{400} after 30 min of incubation, the most effective peptides in the series are WMAP10, W9MAP10, WMAP11, and WMAP12. The eight-residue peptide, WMAP8, was less effective in clearing liposomes and the six-residue peptide, WMAP6, had no discernible effect on lipid. Longer peptides are less effective. The peptide WMAP14 is approximately as effective as the peptide 18As synthesized by Segrest and co-workers (Kanellis et al., 1980). Both WMAP8 and WMAP14 formed optically clear samples within 30 min as judged by eye. W9MAP17, WMAP18, and WMAP6 did not form clear mixtures. Based on the similarity in WMAP10 and W9MAP10, the phase appears to have little bearing on the effectiveness of the peptides in clearing liposomes.

After incubation overnight, most of the mixtures of peptides and either DMPC or DPPC were visually clear. However, WMAP18–DPPC mixtures required mild bath sonication for up to 2 h to become clear before using for spectroscopic measurements or column chromatography. The turbidity of DPPC liposomes without peptide does not change over this time period without sonication. The results of gel filtration chromatography of the peptide–lipid mixtures were consistent with formation of small mixed micelles of peptide and lipid, characteristic of the interaction of amphipathic α-helical peptides and proteins with liposomes (Morrisett et al., 1977). Two examples are in Figure 1, in which the size distribution

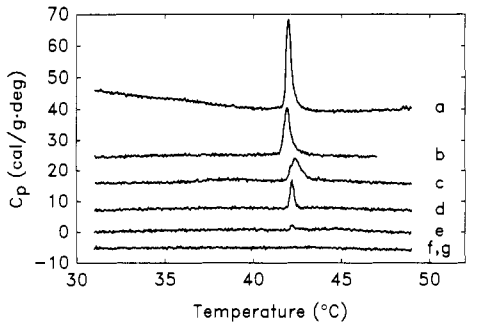

FIGURE 2: Differential scanning calorimetry of (a) DPPC liposomes, (b) WMAP18/DPPC (1:2), (c) W9MAP17/DPPC (1:2), (d) WMAP14/DPPC (1:2), (e) W9MAP10/DPPC (1:2), (f) WMAP10/DPPC (1:2), and (g) WMAP8/DPPC (1:2). Mixtures of peptides and DPPC (1:2 by weight) were prepared by overnight incubation and then scanned at a rate of 1 °C/min at a concentration of 0.1 mg of DPPC/mL.

Table II: Thermal Transitions in DPPC–Peptide Mixtures[a]

mixture	T_m (°C)	ΔH (kcal/mol)	half-width (°C)
DPPC (liposomes)	42.0 ± 0.2	8.7 ± 0.3	0.6
+ WMAP18	41.9 ± 0.2	5.0 ± 0.3	0.9
+ W9MAP17	42.4 ± 0.2	3.2 ± 0.3	1.4
+ WMAP14	42.2 ± 0.2	1.7 ± 0.3	0.5
+ W9MAP10	42.2 ± 0.2	0.4 ± 0.3	0.5
+ WMAP10	43.4 ± 0.2	0.5 ± 0.3	2.0
+ WMAP8	44.5 ± 0.2	0.7 ± 0.3	2.0
+ WMAP6	41.9 ± 0.2	8.9 ± 0.3	0.8

[a] Phase transitions were measured by differential scanning calorimetry. T_m is the midpoint of the main phase transition; ΔH is the enthalpy of the transition; the half-width is the width of the transition at half of the peak heat capacity.

of the micelles is unimodal and the diameter of the micelles increases with increasing lipid/peptide ratio, similar to that observed in mixtures of 18As and DMPC (Anantharamiah et al., 1985; McLean et al., 1989).

Structural Consequences of the Peptide–Lipid Interaction. The effect of peptide on lipid structure was examined by DSC (Figure 2). The T_m and ΔH of the DPPC liposomes were similar to those reported by Phillips (1972). None of the peptides changed T_m by more than 0.4 °C (Table II). However, a dramatic decrease in the enthalpy of the gel to liquid-crystalline phase transition was observed, especially with peptides that were highly effective in clearing DPPC liposomes. As the peptide length decreases, the enthalpy of the transition decreases. In mixtures of W9MAP10 with DPPC at a peptide/lipid weight ratio of 1:2, the phase transition is barely detectable. In mixtures with WMAP10 and WMAP8, the transition is broadened to nearly coincide with the baseline and has an enthalpy of nearly zero. WMAP6 has no effect on the phase transition of DPPC (data not shown).

In the CD, addition of DMPC or DPPC liposomes to the peptides increased the magnitude of the negative bands at 208 and 222 nm in circular dichroism measurements, consistent with an increase in the α-helical contents of the peptides (Figure 3). The addition of TFE, which promotes hydrogen bonding, also increased the α-helicity of the peptides. In the longer peptides (WMAP18, W9MAP17, and WMAP14) and W9MAP10, the α-helicity of the peptide in buffer differs little from that in 80% TFE (Table III). The α-helicity of WMAP10 and WMAP8 is considerably higher in 80% TFE than in water. WMAP6 has little α-helicity under any condition. For the 10-residue peptide, this increase in α-helicity appears to be largely at the expense of β-structure when the spectra are analyzed for α-structure, β-structure, and random

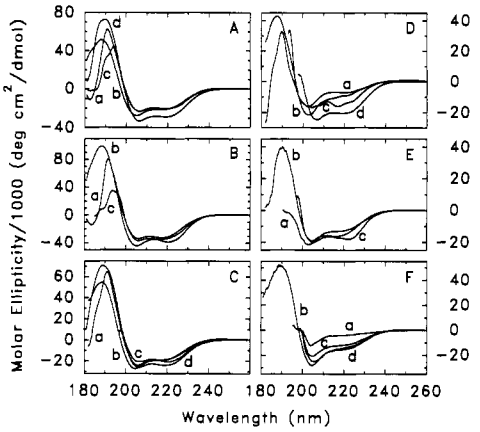

FIGURE 3: CD spectra of peptides in DMPC mixtures. The CD spectra of the peptides were recorded at room temperature at a peptide concentration of 1.7×10^{-5} M. (A) WMAP18; (B) W9MAP17; (C) WMAP14; (D) WMAP10; (E) W9MAP10; (F) WMAP8. In each panel, (a) peptide in buffer, (b) peptide in 80% TFE, (c) peptide/DMPC (1:1), and (d) peptide/DMPC (1:5).

Table III: CD Data on Peptides and Peptide–Lipid Mixtures[a]

peptide	condition	Θ_{208}	Θ_{222}	α_{222}
WMAP18	buffer	−22.4	−19.8	50.9
	80% TFE	−25.2	−19.6	50.3
	+DMPC (1:1)	−22.5	−19.4	49.7
	+DMPC (1:5)	−32.2	−28.0	75.8
W9MAP17	buffer	−32.8	−29.3	79.7
	80% TFE	−41.2	−32.0	87.9
	+DMPC (1:1)	−35.8	−38.1	106.4
WMAP14	buffer	−22.9	−17.7	44.5
	80% TFE	−24.2	−17.7	44.5
	+DMPC (1:1)	−20.5	−20.6	53.3
	+DMPC (1:5)	−25.5	−23.4	61.8
WMAP10	buffer	−9.1	−6.1	9.4
	80% TFE	−13.2	−8.1	15.4
	+DMPC (1:1)	−14.2	−12.4	28.4
	+DMPC (1:5)	−24.3	−20.4	52.6
W9MAP10	buffer	−18.4	−14.3	34.2
	80% TFE	−17.0	−12.0	27.3
	+DMPC (1:1)	−17.2	−18.6	47.4
WMAP9	buffer	−10.7	−5.0	5.9
	80% TFE	−23.9	−13.7	32.4
	+DMPC (1:1)	−17.7	−11.6	26.1
	+DMPC (1:5)	−23.6	−15.1	36.5
WMAP6	buffer	−6.4	−4.1	3.3
	80% TFE	−10.6	−6.1	9.4
	+DMPC (1:1)	−4.7	−3.4	1.2
	+DMPC (1:5)	−8.0	−4.0	3.0

[a] CD spectra were recorded from 250 to 180 nm at a peptide concentration of 0.1 mg/mL and at room temperature. The % α-helix = $-100(\Theta_{222} + 3000)/33000$ (Morrisett et al., 1973).

Table IV: Maximum Fluorescence Emission Wavelength of Peptides and Peptide–Lipid Mixtures[a]

peptide	peptide alone	DMPC (1:1)	DMPC (1:5)
WMAP18	345	341	337
W9MAP17	338	332	332
WMAP14	337	336	336
W9MAP10	352	341	338
WMAP10	346	338	335
WMAP8	354	340	339
WMAP6	350	350	350

[a] Fluorescence spectra were measured at 25 °C and a peptide concentration of 0.1 mg/mL.

structure with the Greenfield and Fasman (1969) parameters. In all of the peptides (except WMAP6), addition of DMPC results in an increase in α-helicity. This increase depends on the lipid/peptide ratio; the α-helical content of the peptides is higher at 1:5 (peptide/lipid) than at 1:1.

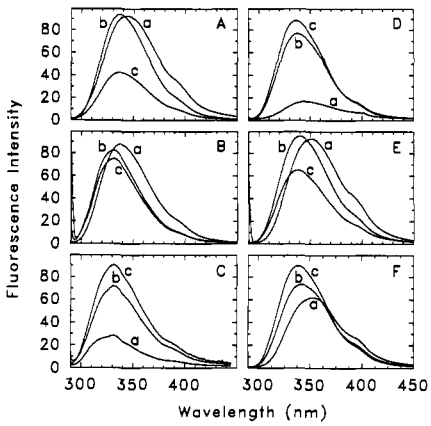

FIGURE 4: Fluorescence spectra of peptides. The samples from the CD experiments were scanned from 290 to 350 nm. (A) WMAP18; (B) W9MAP17; (C) WMAP14; (D) W9MAP10; (E) WMAP10; (F) WMAP8. In each panel, (a) peptide in buffer, (b) peptide/DMPC (1:1), and (c) peptdie/DMPC (1:5).

The effect of DMPC on the environment of the single tryptophan residue of the peptides was examined by fluorescence spectroscopy. Except for W9MAP17 and WMAP14, the tryptophan residue in buffer is relatively solvent-exposed (Table IV). Addition of DMPC liposomes to the peptides results in a blue shift in the fluorescence emission maximum wavelength in all of the peptides that bind to lipid, including WMAP18, but not with WMAP6. The magnitude of the blue shift depends upon the peptide in a manner that appears to be independent of either the effectiveness of the peptide in clearing liposomes or the increase in α-helicity observed on binding lipid. Addition of more DMPC (to attain a 1:5 ratio) increases the blue shift. For WMAP14 and WMAP10, a large increase in the fluorescence intensity with increasing lipid/peptide ratio is also observed (Figure 4).

The fractions of peptide bound to DMPC liposomes were measured under conditions of high dilution and high lipid/peptide ratio. These conditions minimized structural rearrangement of the liposomes and provided sufficient unbound peptide to measure. Peptides were mixed with DMPC liposomes at a concentration of 0.1 mg/mL and a peptide/lipid ratio of 1:50 by weight in a volume of 50 mL. After incubation for 20 h at 24 °C, free peptide was separated from bound peptide by centrifugation at 40000 rpm for 2 h. The pellets and supernatants were separated and concentrated by freeze-drying. Protein concentrations were measured after acid hydrolysis with trinitrobenzenesulfonic acid (McLean & Hagaman, 1989). The percent of peptide bound to the liposomes increased with decreasing peptide length: 25 ± 4% for W9MAP17, 29 ± 4% for WMAP14, 41 ± 4% for WMAP12, and 41 ± 4% for WMAP10 (n = 6–8).

Discussion

A series of novel amphipathic α-helical peptides (MAPs) based on a repeating 11 amino acid sequence were examined for their interaction with phosphatidylcholines. Interaction of amphipathic α-helical peptides with turbid phospholipid liposomes disrupts the structure of the liposomes and produces a clear micellar solution of peptide and lipid (Morrisset et al., 1977). The focus of the present experiments was to determine the minimal sequence requirements for the formation of mixed micelles of a short peptide with lipid. Formation of small, clear mixed micelles of amphipathic α-helical peptides with lipid is correlated with the activity of such lipids as synthetic lung surfactants when mixed with DPPC (McLean et al., 1990). Thus, the primary end point to consider in comparing the peptides is their effectiveness in clearing turbid liposomes. In addition, it is expected that associated with this peptide–lipid interaction is an increase in the α-helicity, a decrease in the solvent exposure of tryptophan, and a decrease in the enthalpy of the phase transition of the lipid (Morrisett et al., 1977). For this, peptides containing from 6 to 18 amino acid residues were utilized. Peptides of 10–12 residues were optimal for the rapid decrease in turbidity of DMPC and DPPC liposomes when mixed at the phase transition temperatures of the lipids; longer peptides were less effective. A peptide of eight residues also formed clear micelles. The peptides that were most effective in disrupting the liposomes and forming clear micelles were also most effective in reducing the enthalpy of the gel to liquid-crystalline phase transition of the lipid. The fraction of peptide that bound to liposomes under conditions in which the liposome structure was minimally perturbed was also higher in the 10 and 12 residue peptides than in the 14 and 17 residue peptides. Consistent with the expected formation of α-helical structure of the peptide upon binding to lipid, addition of DMPC liposomes to the peptides increased the magnitude of the negative bands at 208 and 222 nm in CD measurements. In addition, the fluorescence emission maximum of the single tryptophan residue in the peptides was shifted to shorter wavelengths consistent with transfer of the tryptophan to a less solvent-exposed environment in the presence of lipid. These data demonstrate that an effective lipid-binding amphipathic α-helical peptide need only be eight residues in length.

Several authors have calculated parameters on the basis of peptide sequences to predict the ability of water-soluble peptides to associate with lipid and to form monolayers at the air–water interface. Such surface-associating peptides are generally amphipathic α-helices with high α-helical moments and low hydrophobicities (Pownall et al., 1983; Krebs & Phillips, 1983). In Table V are gathered the primary parameters utilized for quantitatively describing peptide–lipid interactions in amphipathic α-helical peptides. These calculations will be used to help provide a conceptual framework to explain the observed dependence of lipid affinity and clearing on peptide length. Calculations are shown for both the MAP peptides and three literature peptides with well-characterized lipid interactions. The hydrophobicities (H) of the literature peptides span a broad range, which includes that of the MAP series peptides. For the MAP peptides, the total hydrophobicity generally parallels the number of residues in the peptide. The shorter peptides have somewhat lower average hydrophobicities (H_{av}) than the longer MAP peptides. However, 18AS and WMAP14, which are quite effective in clearing and binding to liposomes, have average hydrophobicities equal to or greater than that of WMAP18 or W9MAP17. Thus, a high H_{av} does not necessarily result in a peptide with a rapid rate of clearing or tight binding.

As expected for a series of peptides designed as ideal amphipathic α-helices, the average hydrophobic moments ($\langle H \rangle$) of the MAP peptides are maximal near an angle of 100° per residue, corresponding to an α-helix (Krstenansky et al., 1989), are approximately equal within the series, and are considerably greater in magnitude than those of the model A-I (Fukishima et al., 1979), 18As (Kanellis et al., 1980), or LAP-20 (Pownall et al., 1980) peptides. Inspection of the values of $\langle H \rangle$ and H_{av} show that the MAP peptides have high α-helical moments and low hydrophobicities as expected for surface-associating peptides. Consistent with this are the ratios of the hydrophobic moment to the average hydrophobicity ($\langle H \rangle / H_{av}$), which exceed those of the surface-associating peptides 18As and model A-I. However, the values of $\langle H \rangle / H_{av}$ are not related

Table V: Amphipathic α-Helical Calculations on Peptides[a]

peptide	H	H_{av}	$\langle H \rangle$	$\langle H \rangle / H_{av}$	P/L	α	HI	ion pairs	ΔG_{tr}
WMAP18	−4.09	−0.215	0.420	1.95	1.64	6.7	7.66	4	−19.5
W9MAP17	−2.99	−0.166	0.408	2.46	1.43	3.5	7.05	4	−29.2
WMAP14	−3.43	−0.229	0.413	1.80	1.63	7.3	5.99	3	−10.4
WMAP12	−1.61	−0.124	0.420	3.39	1.35	24.1	5.38	3	−43.4
WMAP11	−2.14	−0.178	0.412	2.32	1.73	24.4	4.77	2	−25.6
WMAP10	−1.14	−0.104	0.427	4.11	1.57	4.2	4.24	2	−28.9
W9MAP10	−1.14	−0.104	0.416	4.00	1.49	9.9	4.24	2	−28.9
WMAP8	−0.95	−0.106	0.417	3.93	1.34	28.0	3.71	2	−34.3
WMAP6	−0.86	−0.122	0.411	3.37	1.48	7.7	2.81	1	−33.3
model A-1[b]	−7.53	−0.342	0.269	0.79	1.00	11.8	8.23	6	−38.1
18As[c]	−4.17	−0.174	0.236	1.36	1.55	6.7	6.65	4	−50.4
LAP-20[d]	−1.86	−0.093	0.272	2.93	0.93	48.1	4.88	2	−68.6

[a] H is the total hydrophobicity of the peptides based on the consensus sequence of Eisenberg et al. (1984). H_{av} is the average hydrophobicity per residue. $\langle H \rangle$ is the per residue magnitude of the hydrophobic moment as defined by Eisenberg et al. (1984) for an α-helix (100° per residue). $\langle H \rangle / H$ is the ratio of the hydrophobic moment to the average hydrophobicity. P/L is the ratio of the projections of the polar (P) and lipophilic (L) moments onto $\langle H \rangle$ (per residue, based on the total number of residues in the peptide), and α is the angle between the hydrophilic and lipophilic moments (Pownall et al., 1983). HI (hydrophobic index) is the sum of the hydrophobicities of the hydrophobic residues on the the nonpolar face of the α-helix (counting Lys as equivalent to Phe) as described by Segrest and Feldmann (1977). The number of potential ion pairs was counted by allowing each acidic or basic residue to participate in no more than one ion pair with a residue at $i + 1$, $i + 3$, or $i + 4$ in an α-helix. The ΔG_{tr} values correspond to the free energy of transfer of random-coil peptide from the aqueous phase to an α-helix completely buried within a hydrophobic phase (von Heijne & Blomberg, 1979). These values do not include the 45–50 kJ/mol free energy increase expected for confining the peptide to a two-dimensional surface. [b] Fukishima et al., 1979. [c] Kanellis et al., 1980. [d] Pownall et al., 1980.

to the clearing efficacy of the peptides. Krebs and Phillips (1983) have stressed the importance of the hydrophobic moment and have correlated surface activity with $\langle H \rangle / F$, where F is the fraction of α-helix in a protein. The shorter MAP peptides are less α-helical in lipid than the longer peptides and, therefore, will have higher $\langle H \rangle / F$ ratios, although this is largely due to end effects within the shorter peptides, which contribute to the reduction in α-helical content of the 10–12 residue peptides. However, the fact that even the longer peptides have high α-helical moments argues against explaining the data in terms of an increase in the α-helical moment operating within the α-helical region of the peptides.

Pownall et al. (1983) have suggested that the ideal lipid-binding peptide would have polar and nonpolar components of the helical moment nearly linear ($\alpha = 0$ in Table V), that the helical moment be exerted near the center of the peptide, and that the polar and nonpolar components of the helical amphipathic moment appear at the same point along the helical axis. For the MAP peptides, the latter two conditions hold because of their regular sequence. However, the value of α varies considerably among the peptides and is not clearly related to their ability to clear lipid. In strongly suface-associating peptides, the ratio of the polar (P) to nonpolar (L) components of the moments (P/L) varies from 0.93 for LAP-20 to 1.6 for 18As, using the Eisenberg consensus scale (Eisenberg et al., 1984) for hydrophobicities. In the MAP series, this ratio is relatively constant and quite high, suggesting that a high P/L value may be important in binding to PC but is not sufficient to explain the relative rates of liposome clearing. Segrest and co-workers (Segrest et al., 1974; Segrest & Feldmann, 1977; Epand et al., 1987) have emphasized the importance of ion pairing in stabilizing interactions between amphipathic α-helical peptides and phosphatidylcholines. This model proposes a specific electrostatic interaction between the charged groups of the peptide and the PC headgroup, which contributes to the stability of the peptide–lipid interactions (Segrest et al., 1974). Mattice and co-workers (Mattice & Robinson, 1981; Hamed et al., 1983) have developed a matrix prediction algorithm based on i to $i + 3$ and i to $i + 4$ ion pairs for predicting α-helical content in proteins bound to lipid. Lipid-binding peptides have been successfully identified from the protein data bank primarily on the basis of ion pairs of the i to $i + 1$, $i + 3$, and $i + 4$ type (Segrest & Feldmann, 1977). Although potential ionic effects may be masked somewhat by the high lipophilicity of the MAP peptides, such potential ionic interactions do not appear to be critical in the MAP series since liposome clearing is not related to either potential salt bridge formation or overall charge (Table V, Krstenansky et al., 1989).

Segrest and Feldmann (1977) also calculated a hydrophobicity index (HI), which corresponds to the total hydrophobicity of the residues on the nonpolar face of the amphipathic α-helix plus a contribution from the Lys hydrocarbon region. These calculations stress the importance of the hydrophobic effect in driving membrane association. A similar calculation was made (Table V) of the total hydrophobicity of the nonpolar residues (which all lie on the nonpolar face in the MAP peptides) and includes a contribution from Lys residues equal to the hydrophobicity of Phe as in Segrest and Feldmann (1977). Pownall et al. (1983) also stress the critical importance of nonpolar residues in the peptide–lipid interaction for amphipathic α-helical peptides and suggest that the hydrophobicity of the hydrophobic face determines to a significant degree the energetics of transfer of the peptide from water to an interface. The data of Table V indicate that the peptides with the highest HI are the poorest for liposome clearing and binding. In fact, for the series of peptides containing from 10 to 18 residues, the efficacy of clearing correlates with a decrease in hydrophobic index. A stepwise linear regression analysis of the data in Table V for this range of peptide lengths indicates that the strongest predictor of lipid clearing is a low hydrophobic index. However, a minimum hydrophobic index of ~4 appears to be required to elicit any interaction with lipid.

On the basis of the success of the hydrophobic index in predicting the efficacy of liposome clearing, an approach based on calculating free energies of binding from the size of the hydrophobic surface areas of the peptides was made. Only the hydrophobic side chains of the amino acid residues were considered, including contributions from the Lys and Glu residues (Figure 5). For this series of peptides an optimal hydrophobic surface area of 6–7.5 nm^2 is observed for liposome clearing, somewhat larger than the 4.6-nm^2 area of the two acyl chains of DPPC. Assuming a free energy of transfer of 10.1 (kJ/mol)/nm^2 of hydrophobic surface (Chothia, 1974), the optimal peptides will gain 60–75 kJ/mol when transfered to a nonpolar phase. This may be compared with the unfavorable 45–50 kJ/mol free energy change associated with confining the peptide to two dimensions in the surface of the

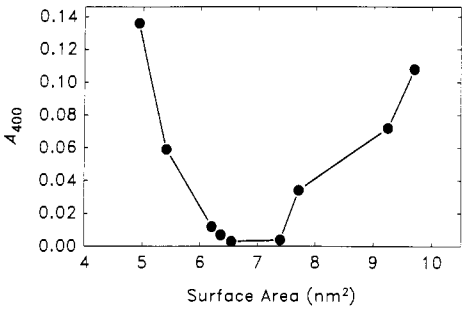

FIGURE 5: Relationship between the rate of liposome clearing and the hydrophobic surface area of the peptides. Molecular models of the peptides were constructed with INSIGHT (BioSym) software operating on a PS-300 interfaced to a VAX 11-780. Calculations of the solvent-accessible surface area were made with the same software, assuming a probe radius of 0.2 nm. This gives the surface area of the peptide that is accessible to the probe rolling over the surface. The area calculation was restricted to the hydrophobic regions of the peptides by considering only the side-chain atoms of Leu, Mpa, and Trp, the carbon β to the peptide backbone in Glu and Suc, and the carbons β and γ to the peptide backbone in Lys and 6-Ahx along with their associated hydrogens. The atoms within the peptide backbone, the terminal amide, and the two carbons adjacent to the charged oxygen and nitrogen of Glu (Suc) and Lys (6-Ahx), respectively, were considered as hydrophilic and were not included in the surface area calculation.

liposome or micelle (Janin & Chothia, 1978; McLean & Phillips, 1984; von Heijne & Blomberg, 1979; Schwyzer, 1986). Peptides with a surface ΔG_{tr} insufficient to compensate for this unfavorable entropy loss on binding are not expected to bind to lipid. Thus, peptides such as WMAP8 and WMAP6 would not be expected to bind with high affinity to lipid. However, the ΔG_{tr} of the entire peptide to a hydrophobic phase (Table V) is insufficient for complete burial of the peptide. These calculations suggest a lower limit of $\sim$10 residues for interfacial binding of this series of peptides.

The inefficient clearing of liposomes observed upon addition of longer peptides may be the result of a low affinity of these peptides for lipid. The limited binding data reported here support such a contention. However, on the basis of the hydrophobic indices of the peptides (Table V and Figure 5) there is no a priori reason to expect low liposome affinity in the longer peptides. Several possibilities for the low affinity and minimal clearing activity of the longer peptides may be considered. In 1981, Massey et al. showed that the association of apoA-I with DMPC proceeds more rapidly when the protein is added in GdnHCl. We have also shown that activation of lipoprotein lipase by apoC-II is not effective when the peptide is not added in GdnHCl (McLean et al., 1986). These results appear to be due to the relatively slow rate of association of aggregated apolipoproteins with PC; in GdnHCl, the proteins are added to the liposome suspension as monomers. In the present set of experiments, all peptides were added to liposomes from a GdnHCl solution in which the peptides take on a random structure based on CD (L. R. McLean, unpublished results), suggesting a monomeric state. Thus, the slow rate of clearing for the longer MAP peptides is not due to addition of aggregated peptide.

A second possibility is based on the observation that the rate of association of apoA-I with lipid depends upon the aggregation state of the apolipoprotein (Massey et al., 1981). On the basis of this argument, smaller peptides would associate more rapidly with lipid because a larger number of suitably sized holes into which the peptide can insert are available in the bilayer. For penetration of a monolayer, the activation energy barrier for clearing a hole of area X is $E = \langle\pi\rangle X$, where $\langle\pi\rangle$ is the average surface pressure (Phillips et al., 1975). For a bilayer $\langle\pi\rangle \sim 20$ mN/m and for the 10-residue peptide $X \sim 2.4$ nm^2 (based on molecular models). Thus, $E \sim 2.4$ kJ/mol for the shortest optimal peptide. For the 18-residue peptide, the larger hole size ($X \sim 4.1$ nm^2) required to accommodate the peptide results in a higher activation energy barrier for penetration of the liposome monolayer ($E \sim 4.1$ kJ/mol). These energy barriers are relatively small but are markedly influenced by the compressibility of the bilayer and will depend upon the peptide/lipid ratio in the micelle (McLean et al., 1989). The precise relationship between peptide size and the rate of bilayer hole formation is not clear, but such notions might be extended to present an intriguing hypothesis to explain the data.

Another hypothesis that may explain the relatively low liposome affinity and clearing rate for the longer MAP peptides takes into account the complex nature of the kinetics of clearing, which consists of (1) binding of the peptide to the bilayer, (2) self-association of the peptide, and (3) restructuring of the liposomes into disks. The lower lipid affinity of the longer peptides argues against the third process as the primary determinant of the observed dependence on peptide length. However, the effectiveness of any particular peptide in clearing liposomes may depend on the rate of restructuring of the liposomes to disks. Considering the first and second processes, increasing the size of the hydrophobic face is not only expected to increase the affinity for lipid but may also increase the affinity of the peptide for itself. In both cases, dehydration of the hydrophobic side chains is the primary driving force for association [cf. deGrado and Lear (1985)], but ionic interactions cannot be ruled out. Thus, when the peptide is added to the liposome suspension, peptide–peptide interactions may be thermodynamically favored over peptide–lipid interactions for longer peptides. It is not clear how such interactions may contribute to the kinetics, but considering peptide binding data solely in terms of affinities of peptide for lipid may ignore the possibility of peptide–peptide interactions. Clearly, further experimental data are required to separate the contributions of peptide self-association, bilayer hole formation, and liposome restructuring to the kinetics of the association of amphipathic α-helical peptides with phosphatidylcholines.

Registry No. DPPC, 63-89-8; DMPC, 18194-24-6; WMAP18, 130468-42-7; W9MAP17, 130468-43-8; WMAP14, 130468-44-9; WMAP12, 130468-45-0; WMAP11, 130468-46-1; WMAP10, 130468-47-2; W9MAP10, 130468-48-3; WMAP8, 130468-49-4; WMAP6, 130468-50-7.

REFERENCES

Anantharamaiah, G. M., Jones, J. L., Brouillette, C. G., Schmidt, C. F., Chung, B. H., Hughes, T. A., Bhown, A. S., & Segrest, J. P. (1985) *J. Biol. Chem. 260*, 10248–10255.

Argiolas, A., & Pisano, J. J. (1985) *J. Biol. Chem. 260*, 1437–1444.

Chothia, C. (1974) *Nature 248*, 338–339.

deGrado, W. F., & Lear, J. D. (1985) *J. Am. Chem. Soc. 107*, 7684–7689.

Eisenberg, D., Weiss, R. M., & Terwilliger, T. C. (1984) *Proc. Natl. Acad. Sci. U.S.A. 81*, 140–144.

Epand, R. M., Gawish, A., Iqbal, M., Gupta, K. B., Chen, C. H., Segrest, J. P., & Anantharamaiah, G. M. (1987) *J. Biol. Chem. 262*, 9389–9396.

Fukishima, D., Kupferberg, J. P., Yokoyama, S., Kroon, D. J., Kaiser, E. T., & Kezdy, F. J. (1979) *J. Am. Chem. Soc. 101*, 3703–3704.

Greenfield, N., & Fasman, G. D. (1969) *Biochemistry 8*, 4108–4116.

Hamed, M. M., Robinson, R. M., & Mattice, W. L. (1983) *Biopolymers 22*, 1003-1021.
Janin, J. & Chothia, C. (1978) *Biochemistry 17*, 2943-2948.
Kaiser, E. T., & Kezdy, F. J. (1984) *Science 223*, 249-255.
Kanellis, P., Romans, A. Y., Hohnson, B. J., Kercret, H., Chisvetti, R., Jr., Allen, T. M., & Segrest, J. P. (1980) *J. Biol. Chem. 255*, 11464-11472.
Krebs, K. E., & Phillips, M. C. (1983) *Biochim. Biophys. Acta 754*, 227-230.
Krstenansky, J. L., Owen, T. J., Hagaman, K. A., & McLean, L. R. (1989) *FEBS Lett. 242*, 409-413.
Massey, J. B., Gotto, A. M., Jr., & Pownall, H. J. (1981) *Biochim. Biophys. Res. Commun. 99*, 466-474.
Mattice, W. L., & Robinson, R. M. (1981) *Biopolymers 20*, 1421-1434.
McLean, L. R., & Phillips, M. C. (1984) *Biochemistry 23*, 4624-4630.
McLean, L. R., & Hagaman, K. A. (1989) *Biochemistry 28*, 321-327.
McLean, L. R., Demel, R. A., Socorro, L., Shinomiya, M., & Jackson, R. L. (1986) *Methods Enzymol. 129*, 738-763.
McLean, L. R., Krstenansky, J. L., Owen, T. J., Eftink, M. R., & Hagaman, K. A. (1989) *Biochemistry 28*, 8403-8410.
McLean, L. R., Krstenansky, J. L., Lewis, J. E., Jackson, R. L., Hagaman, K. A., Matthews, E. R. & Owen, T. J. (1990) *Am. Rev. Resp. Dis. 141*, A538.
Morrisett, J. D., Jackson, R. L., & Gotto, A. M., Jr. (1977) *Biochim. Biophys. Acta 472*, 93-133.
Phillips, M. C. (1972) *Prog. Surf. Membr. Sci. 5*, 139-221.
Phillips, M. C., Graham, D. E., & Hauser, H. (1975) *Nature 254*, 154-155.
Pownall, H. J., Hu, A., Albers, J. J., Gotto, A. M., Jr., & Sparrow, J. T. (1980) *Proc. Natl. Acad. Sci. U.S.A. 77*, 3154-3158.
Pownall, H. J., Knapp, R. D., Gotto, A. M., Jr., & Massey, J. B. (1983) *FEBS Lett. 159*, 17-23.
Schwyzer, R. (1986) *Biochemistry 25*, 4281-4286.
Segrest, J. P., & Feldmann, R. J. (1977) *Biopolymers 16*, 2053-2065.
Segrest, J. P., Jackson, R. L., Morrisett, J. D., & Gotto, A. M., Jr. (1974) *FEBS Lett. 38*, 247-253.
Srinivas, R. V., Birkedal, B., Owens, R. J., Anantharamaiah, G. M., Segrest, J. P., & Compans, R. W. (1990) *Virology 176*, 48-57.
von Heijne, G., & Blomberg, C. (1979) *Eur. J. Biochem. 97*, 175-181.

Rhodopsin in Dimyristoylphosphatidylcholine-Reconstituted Bilayers Forms Metarhodopsin II and Activates G_t[†]

Drake C. Mitchell, Julia Kibelbek, and Burton J. Litman*
Department of Biochemistry, University of Virginia Health Sciences Center, Charlottesville, Virginia 22908
Received July 30, 1990; Revised Manuscript Received September 24, 1990

ABSTRACT: The photochemical intermediate metarhodopsin II (meta II; λ_{max} = 380 nm) is generally identified with rho*, the conformation of photolyzed rhodopsin which binds and activates the visual G-protein, G_t [Emeis, D., & Hoffman, K. P. (1981) *FEBS Lett. 136*, 201-207]. Purified bovine rhodopsin was incorporated into vesicles consisting of dimyristoylphosphatidylcholine (DMPC), and the rapid formation of a photochemical intermediate absorbing maximally at 380 nm was quantified via both flash photolysis and equilibrium spectral measurements. Kinetic and equilibrium spectral measurements performed above the T_m of DMPC showed that G_t, in the absence of GTP, enhances the production of the 380-nm-absorbing species while reducing the concentration of the 478-nm-absorbing species, metarhodopsin I (meta I), in a manner similar to that observed in the native rod outer segment disk membrane. This G_t-induced shift in the equilibrium concentration of photointermediates indicated that the species with an absorbance maximum at 380 nm was meta II. The presence of rho* in the DMPC bilayer was established via measurements of photolysis-induced exchange of tritiated GMPPNP, a nonhydrolyzable analogue of GTP, on G_t. Above T_m, the metarhodopsin equilibrium is strongly shifted toward meta I relative to the native rod outer segment disk membrane; however, at 37 °C, 40% of the photointermediates are in the form of meta II. The formation of meta II above T_m is slowed by a factor of ca. 2 relative to the disk membrane. Below T_m, the equilibrium is shifted still further toward meta I, and meta II forms ca. 7 times slower than in the disk membrane. Below T_m, photolyzed rhodopsin was still capable of activating G_t, although the rate was about 12× slower than that observed above T_m, confirming the presence of meta II in the gel-phase bilayer.

The visual pigment rhodopsin of the disk membrane of the vertebrate rod outer segment is an integral membrane protein consisting of hydrophilic domains linked by seven α-helices which span the disk membrane (Ovchinikov, 1982; Hargrave et al., 1983). Rhodopsin is representative of the class of integral membrane protein receptors which accomplish their signal transduction function by activating a specific G-protein. This combination of signal transduction by means of a ubiquitous mechanism and intimate contact with the phospholipid bilayer makes rhodopsin an ideal subject for studying the effects of bilayer composition and physical properties on signal transduction by integral membrane proteins.

[†]Supported by NIH Grant EY00548. A previous report of this work appeared in Mitchell et al. (1990a).
* Author to whom correspondence should be addressed.

0006-2960/91/0430-37$02.50/0